

# Original Research Article

## Synergistic Design of $\text{Co}_3\text{O}_4$ Nanoparticles for Advanced Supercapacitor Electrodes: Hydrothermal Synthesis, Characterization, and Performance Evaluation

### ABSTRACT

The potential of cobalt oxide ( $\text{Co}_3\text{O}_4$ ) nanoparticles, synthesized via a facile hydrothermal method, as electrode materials for supercapacitors is investigated in this research. Through a comprehensive characterization approach involving X-ray diffraction (XRD), Fourier-transform infrared spectroscopy (FT-IR), scanning electron microscopy (SEM), surface wettability analysis, and Brunauer-Emmett-Teller (BET) analysis, the structural and morphological properties of the synthesized  $\text{Co}_3\text{O}_4$  nanoparticles were thoroughly examined. XRD analysis confirmed the presence of the cubic phase of  $\text{Co}_3\text{O}_4$ , while FT-IR spectroscopy revealed the characteristic Co-O bonds. SEM imaging showcased the non-uniform aggregation of nanoparticles. BET analysis provided crucial insights into surface area and pore radius parameters. Notably,  $\text{Co}_3\text{O}_4$  nanoparticles exhibited hydrophilic behavior. In the presence of KOH electrolyte,  $\text{Co}_3\text{O}_4$ -carbon cloth (CC) electrodes demonstrated exceptional specific capacitances ( $C_s$ ) of  $132 \text{ Fg}^{-1}$  in KOH and  $79 \text{ Fg}^{-1}$  in  $\text{Na}_2\text{SO}_4$ , coupled with outstanding cycling stability ( $\sim 75\%$  retention after 500 cycles) in KOH, underscoring their potential as promising electrode materials for supercapacitor applications.

*Keywords: Nanotechnology,  $\text{Co}_3\text{O}_4$  nanoparticles, Hydrothermal Method, Characterization, Supercapacitor Application*

### 1. INTRODUCTION

Nanoparticles' special qualities and wide range of uses have made them indispensable in many scientific and technical domains[1]. Exact control over the production and design of nanoparticles with specific properties has been made possible by nanotechnology, which is the manipulation and engineering of materials at the nanoscale[2]. These nanoscale structures are essential in a variety of fields, including electronics, medicine, catalysis, and energy storage, because they display unique physical, chemical, and biological characteristics[3].

Nanotechnology has completely changed the energy storage market by providing creative answers to the growing need for effective and environmentally friendly energy storage technologies[4]. Supercapacitors are one of these alternatives that has attracted a lot of attention because of its high power density, quick charging and discharging speed, and extended cycle life[5]. Supercapacitors are essential components of contemporary energy systems, finding use in anything from electric automobiles and portable devices to grid-level energy storage[6].

In an attempt to improve the efficiency of supercapacitors, scientists are investigating new electrode materials, and nanoparticles have surfaced as a serious candidate[7]. To increase the energy storage capacity and electrochemical performance of supercapacitors, nanoparticles with special properties including high surface area, variable porosity, and superior electrical conductivity are greatly desired. Scientists hope to advance supercapacitor technology toward greater dependability and efficiency by utilizing the advantages of nanoparticles[8].

$\text{Co}_3\text{O}_4$  nanoparticles can be made using a variety of techniques, including as hydrothermal synthesis, chemical vapor deposition (CVD), sputtering, electrochemical processes, hydrothermal synthesis, sol-gel synthesis, and chemical bath deposition[9]. The capacity to create  $\text{Co}_3\text{O}_4$  nanoparticles with various morphologies and structures which can greatly improve their electrochemical properties, makes hydrothermal synthesis stand out among these techniques[10].

A variety of techniques, including sol-gel, hydrothermal, and chemical vapor deposition, are commonly used in the production of nanoparticles, including  $\text{Co}_3\text{O}_4$ [11]. Each technique has certain benefits with regard to control over size, shape, and crystallinity. In particular, hydrothermal synthesis has become more and more popular because of its ease of use, scalability, and capacity to provide nanoparticles with consistent morphology and size[12]. This process creates nanoparticles with the required characteristics by reacting precursor materials in an aqueous solution at high pressures and temperatures[12].

In order to understand the structural, morphological, and electrochemical characteristics of nanoparticles and whether or not they are suitable for a given application, characterization procedures are essential. X-ray diffraction (XRD), scanning electron microscopy (SEM), Fourier-transform infrared spectroscopy (FTIR), and electrochemical impedance spectroscopy (EIS) are examples of common characterisation techniques. By examining the crystal structure, surface morphology, chemical makeup, and electrochemical activity of nanoparticles, researchers can better optimize synthesis procedures and create materials that are specifically suited for intended uses[13].

One interesting way to improve the performance of supercapacitors is to use  $\text{Co}_3\text{O}_4$  nanoparticles as the electrode material[14].  $\text{Co}_3\text{O}_4$  nanoparticles are ideally suited for effective energy storage due to their high specific capacitance, great chemical stability, and outstanding electrical conductivity. Furthermore, the development of supercapacitors with improved energy density, power density, and cycling stability is made possible by the special qualities of  $\text{Co}_3\text{O}_4$  in combination with the benefits of electrode designs based on nanoparticles[15]. Through the utilization of sophisticated electrode design methodologies and the synergistic impacts of nanoscale materials, researchers hope to fully realize the promise of  $\text{Co}_3\text{O}_4$  nanoparticles for next-generation supercapacitor technologies. Comparing  $\text{Co}_3\text{O}_4$  to other metal oxides, there are several benefits: low toxicity, economical, high chemical and thermal stability, readily available, and environmentally benign[16].  $\text{Co}_3\text{O}_4$  is a good option for energy storage applications because of its substantial theoretical specific capacitance (Cs) within a potential window of 0.5 V[15].

Batteries, power modules, and electrochemical capacitors (supercapacitors) are among the most practical and beneficial developments for electrochemical energy storage and processing in a variety of applications[17]. Because of their high energy thickness, excellent charge-release rate, extended cycle life (more than 5,000 000 cycles), excellent stability, and wide range of applications such as power reinforcement systems, lightweight, versatile devices, and hybrid electric vehicles supercapacitors have become increasingly commonplace in recent years[18].

This work focuses on synthesizing  $\text{Co}_3\text{O}_4$  nanoparticles using a straightforward hydrothermal technique and examines their electrochemical characteristics in several electrolytes, including sodium sulfate ( $\text{Na}_2\text{SO}_4$ ) and potassium hydroxide (KOH). One can learn more about the applicability and potential of  $\text{Co}_3\text{O}_4$  nanoparticles for supercapacitor applications by methodically examining their performance as electrode materials in different electrolytes.

Due to the growing global interest in energy, the rapidly expanding global economy, the decline in the use of petroleum derivatives, the growing concern over environmental issues, the growing need for convenient electronic devices, and the rising popularity of crossover vehicles, there is an urgent need for clean, sustainable, eco-friendly, high energy stockpiling and transformation innovation[19].

## **2. EXPERIMENTAL DETAILS**

### **2.1 Synthesis of $\text{Co}_3\text{O}_4$ powder by Hydrothermal route**

A set of procedures was followed in the hydrothermal synthesis of  $\text{Co}_3\text{O}_4$  nanoparticles in order to create porous  $\text{Co}_3\text{O}_4$  powder. Every reagent used in the synthesis procedure was of analytical quality. The standard protocol involved adding 1 mol of cobaltacetate  $\text{Co}(\text{CH}_3\text{CO}_2)_2 \cdot 4\text{H}_2\text{O}$  to a combination of 5 ml of double-distilled water and 15 ml of methanol, then continuously swirling with a magnetic stirrer for 15 minutes. After being fully dissolved, the transparent solution was put into a 20 ml Teflon container and heated to  $125^\circ\text{C}$  for four hours using hydrothermal treatment. After letting the autoclave cool naturally, the finished product was gathered and thoroughly cleaned with ethanol and water to get rid of any remaining impurities. The powder that had been gathered was then heated to  $60^\circ\text{C}$  and then calcined for two hours at  $350^\circ\text{C}$  in an airtight environment[20].

### **2.2 Preparation of working electrode**

A mixture of 80 weight percent  $\text{Co}_3\text{O}_4$  electro-active material, 10 weight percent carbon black, and 10 weight percent PVDF binder (polyvinylidene difluoride) in NMP solvent (1-methyl-2-pyrrolidinone) was premixed to create the working electrode. After the combination was well mashed to guarantee homogeneity, the resultant slurry was applied to a  $1 \times 1 \text{ cm}^2$  flexible carbon cloth (CC) substrate. The coated electrode's mass loading of active materials was kept constant at  $41.8 \text{ mgcm}^{-2}$ . The coated electrode was then dried at  $60^\circ\text{C}$  to eliminate any remaining solvent and promote the active components' adherence to the carbon cloth substrate[21].

This method of manufacture guaranteed even dispersion of the  $\text{Co}_3\text{O}_4$  nanoparticles in the electrode matrix, promoted electron transport, and gave the electrode mechanical stability. The electrode's overall electrochemical performance and electrical conductivity were both improved by the addition of carbon black. Furthermore, by adhering the active components to the carbon cloth substrate, PVDF binder helped to prevent their separation during electrochemical cycling[22]. The resulting  $\text{Co}_3\text{O}_4$ -based working electrode showed superior electrical conductivity[23], effective charge transfer kinetics, and a high specific surface area, all of which are desirable properties for supercapacitor applications[24].

Due to these characteristics, the electrode can be used in high-end supercapacitor systems that provide improved long-term cycle stability and energy storage[25].

### 3. CHARACTERIZATION OF NANOPARTICLES

#### 3.1 FTIR

Using infrared spectroscopy, the chemical bonding properties of materials are assessed. The FT-IR spectra of the as-prepared nanocrystalline  $\text{Co}_3\text{O}_4$  made by hydrothermal decomposition of cobaltacetate  $\text{Co}(\text{CH}_3\text{CO}_2)_2 \cdot 4\text{H}_2\text{O}$ [26]. In addition to the prominent bands indicating the presence of  $\text{Co}_3\text{O}_4$  spinel oxide and the vibrational modes associated with its chemical bonding, further insights can be gleaned from the infrared spectroscopic analysis of the as-prepared nanocrystalline  $\text{Co}_3\text{O}_4$ . The observed peaks at approximately  $660\text{ cm}^{-1}$  and  $570\text{ cm}^{-1}$  correspond to the  $\nu(\text{CoO})$  vibrational modes, which signify the stretching vibrations of the cobalt-oxygen bonds within the crystal lattice. These peaks serve as unequivocal evidence for the formation of the desired  $\text{Co}_3\text{O}_4$  phase through the hydrothermal decomposition process employed. Furthermore, the broad absorption band centered at around  $3424\text{ cm}^{-1}$  can be attributed to the O-H stretching vibrations of water molecules adsorbed onto the surface of the nanoparticles. This phenomenon is common in materials synthesized via wet chemical methods, such as hydrothermal synthesis, where residual water molecules often remain entrapped within the nanostructure. Similarly, the weak absorption peak at  $1618\text{ cm}^{-1}$  corresponds to the bending vibrations of adsorbed water molecules, further confirming the presence of surface-bound water species. The detection of these water-related peaks underscores the need for thorough characterization and understanding of the surface chemistry in nanomaterial synthesis[27].

Overall, the FT-IR analysis provides valuable insights into the chemical composition and bonding properties of the  $\text{Co}_3\text{O}_4$  nanoparticles, crucial for elucidating their structure-property relationships and informing their potential applications in various fields, including catalysis, sensing, and energy storage[26].

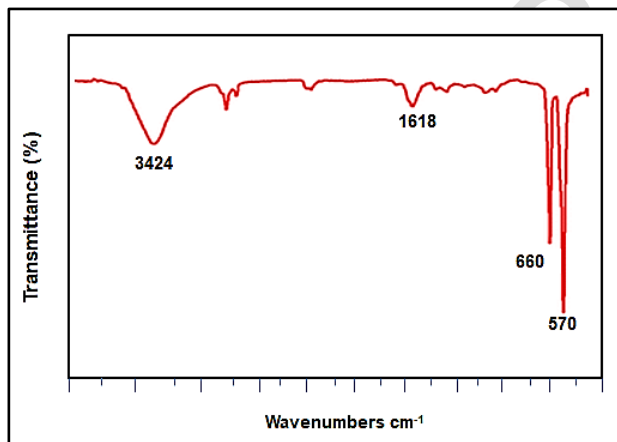


Fig.1 FTIR Spectra of  $\text{Co}_3\text{O}_4$  Nanoparticles

#### 3.2 XRD

The XRD pattern of the synthesized  $\text{Co}_3\text{O}_4$  nanoparticles revealed distinct diffraction peaks at specific  $2\theta$  angles, indicative of their crystalline nature and structural properties[28]. The peaks corresponding to the (110), (222), (520), (190), (400), and (422) crystallographic planes were observed at  $2\theta$  angles of  $19.01^\circ$ ,  $32.34^\circ$ ,  $60.53^\circ$ ,  $21.87^\circ$ ,  $44.67^\circ$ , and  $56.32^\circ$ , respectively. Each peak's position and intensity provide valuable information about the crystal structure and phase composition of the material[28]. The sharp, well-defined peaks suggest a high degree of crystallinity and phase purity, consistent with the formation of phase-pure  $\text{Co}_3\text{O}_4$ . This observation is further supported by the absence of additional peaks associated with impurity phases, as verified by comparison with the standard JCPDS No. 76-1802. Phase pure  $\text{Co}_3\text{O}_4$  has formed, as confirmed by the lack of diffraction peaks associated with CoO and other phases[29]. This is consistent with standard JCPDS No. 76-1802. Using the Debye-Scherrer equation

$$0.9 D = (\cos \lambda) / (\beta \theta) \quad \text{eq.1}$$

where  $\lambda$  is the wavelength of Cu- $\alpha$  radiation ( $1.5418 \text{ \AA}$ ),  $\beta$  is the full width half-maximum (FWHM) in radians, and  $\theta$  is the angle of diffraction (in radians), the average crystallite size was determined.

$\beta$  (FWHM in radians) = convert from degrees to radians

$\theta$  (angle of diffraction in radians) = convert from degrees to radians

Let's say for the (110) peak at  $2\theta = 19.01^\circ$ :

Convert  $2\theta$  from degrees to radians:  $\theta = 19.01^\circ \times \pi/180 \approx 0.332$  radians

Convert FWHM from degrees to radians:  $\beta = 0.1^\circ \times \pi/180 \approx 0.00175$  radians

Now, plug these values into the equation:

$$0.9 D = (\cos \lambda) / (\beta * \theta)$$

$$D \approx (\cos 1.5418) / (0.00175 * 0.332)$$

Calculating:

$$D \approx (0.02055) / (0.000581)$$

$$D \approx 35.38 \text{ \AA (angstroms)}$$

So, for the (110) peak at  $2\theta = 19.01^\circ$ , the estimated average crystallite size is approximately 35.38 angstroms.

This process can be repeated for each diffraction peak observed in the XRD pattern to obtain the average crystallite size corresponding to different crystallographic planes, providing comprehensive insight into the nanostructural characteristics of the  $\text{Co}_3\text{O}_4$  nanoparticles. The peak positions correspond to specific lattice planes within the face-centered cubic spinel structure of  $\text{Co}_3\text{O}_4$ , as described by the  $Fd\bar{3}m$  space group. The (110) peak at  $19.01^\circ$ , for instance, represents the interplanar spacing of the (110) crystallographic planes, while the (222) peak at  $32.34^\circ$  corresponds to the (222) planes, and so forth.

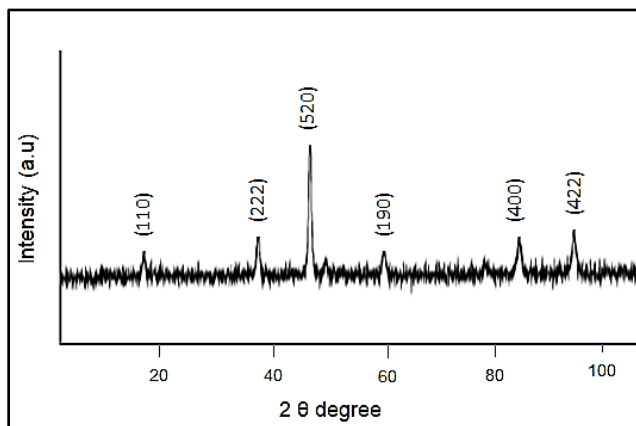


**Fig.2 XRD Pattern of  $\text{Co}_3\text{O}_4$  Nanoparticles**

### 3.3 SEM

The shape and size distribution of the  $\text{Co}_3\text{O}_4$  nanoparticles, which were created by hydrothermally breaking down the cobalt acetate precursor, are better understood according to the SEM study[30]. The nanoparticles' asymmetrical form and surface characteristics are visible in the SEM pictures, which are a reflection of their complex growth mechanism and surface interactions during synthesis[31].

Furthermore, the  $\text{Co}_3\text{O}_4$  nanoparticles' homogeneity and narrow size distribution, which ranges from 20 to 150 nm are shown in the SEM pictures. This uniform distribution of particle sizes is a sign of the regulated kinetics of nucleation and growth that are attained in hydrothermal settings, where temperature, pressure, and concentration of precursors are important variables that affect the final morphology of the nanostructure[32].

Furthermore, the observed sizes of the nanoparticles within the given range are very desirable for a variety of applications, such as energy storage, sensing, and catalysis, where the performance of the particles is often determined by their size. Through hydrothermal synthesis,  $\text{Co}_3\text{O}_4$  nanoparticles' size and morphology may be accurately controlled, providing chances to modify their properties to suit particular application needs[33].

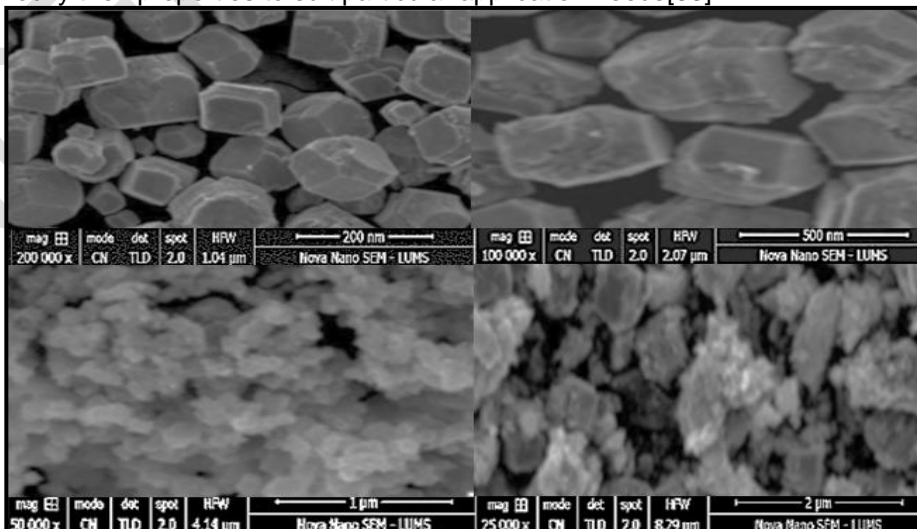


**Fig.3 SEM micrographs of  $\text{Co}_3\text{O}_4$  Nanoparticles at different resolution of  $1\mu\text{m}$ ,  $2\mu\text{m}$ ,  $200\text{nm}$  and  $500\text{nm}$**

### 3.4 BET characterization

BET characterization was done to look at the surface properties of the  $\text{Co}_3\text{O}_4$  nanoparticles[34]. The  $\text{Co}_3\text{O}_4$  adsorption–desorption isotherms for  $\text{Co}_3\text{O}_4$  and the corresponding pore size distribution, which was investigated with the Barrett–Joyner–Halenda (BJH) method[35], are depicted in the figure.  $\text{Co}_3\text{O}_4$  nanoparticle isotherms in the 0–1 high relative pressure ( $P/P_0$ ) range exhibit a hysteresis loop. The slope in the presented figure grows from 0.4 to 0.9 at high relative pressures, suggesting that the material is mesoporous.

The maximum BET surface area for  $\text{Co}_3\text{O}_4$  nanoparticles was found to be  $28.4 \text{ m}^2/\text{g}$ . Within their nanocluster structure,  $\text{Co}_3\text{O}_4$  nanoparticles have an average pore radius of 17.5 nm in the porous zone.  $\text{Co}_3\text{O}_4$  nanoparticles' porous nanocluster form improves reaction kinetics by offering porosity, more active sites, and rapid charge-discharge capabilities. This makes them useful in applications such as supercapacitors.

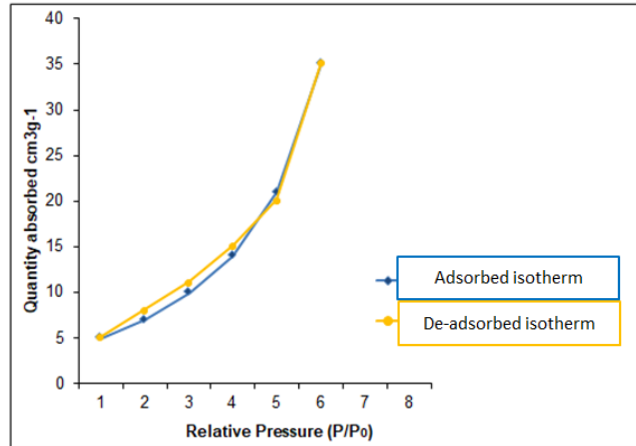


**Fig.4 CoO adsorption–desorption isotherms for  $\text{Co}_3\text{O}_4$**

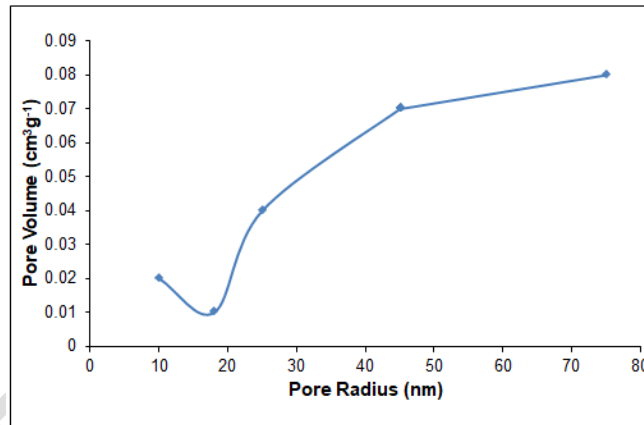


**Fig.5 Plot of pore volume vs. pore radius**

### 3.5 Surface Wettability Test

Surface wettability was assessed to look at how the  $\text{Co}_3\text{O}_4$  electrode and the electrolyte interacted [36]. A large contact angle ( $\theta > 90^\circ$ ), indicating a hydrophobic surface, suggests lower wettability [37]. Conversely, a short contact angle ( $\theta < 90^\circ$ ) indicates a hydrophilic surface and suggests more wettability. Hydrophilic materials usually show high surface energy. In this experiment, the contact angle between the water and the  $\text{Co}_3\text{O}_4$  electrode surface was discovered to be  $52^\circ$ , as seen in the accompanying figure. One essential characteristic of nanocrystalline materials intended for use as supercapacitor electrodes is hydrophilicity. This result is in line with studies that looked at the hydrophilic properties of copper oxide multilayer nanosheets [38].

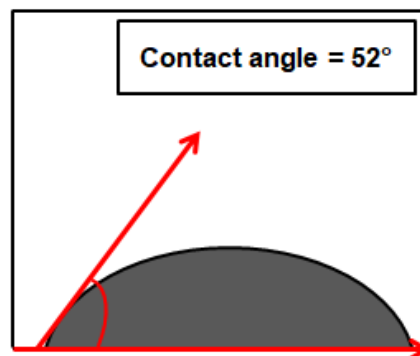


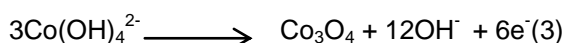
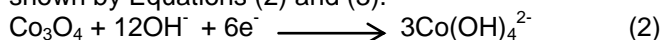
**Fig.6 Static contact angle measurement of CoO electrode**

## 4. Electrochemical Measurements

### 4.1 Electrochemical Measurements of Co<sub>3</sub>O<sub>4</sub> Nanoparticles as Electrode

The Co<sub>3</sub>O<sub>4</sub> nanoparticle electrode was electrochemically characterized using a conventional three-electrode setup. The electrode arrangement consisted of a platinum counter electrode, a SCE (Standard Calomel Electrode) reference electrode, and a Co<sub>3</sub>O<sub>4</sub> nanoparticle working electrode[39]. For the measurements, one million KOH alkaline solution and one million Na<sub>2</sub>SO<sub>4</sub> neutral solution were utilized.

The CV curves in KOH electrolyte at a scan rate of 5 mVs<sup>-1</sup> for both bare carbon cloth (CC) and CC modified by Co<sub>3</sub>O<sub>4</sub> nanoparticles are displayed in given figure. An oxidation peak, associated with the transformation of Co<sub>3</sub>O<sub>4</sub> into CoOOH, is observed at around 0.42 V. At roughly 0.27 V, the decrease peak appears as a result of the opposite reaction. When compared to the naked CC, the Co<sub>3</sub>O<sub>4</sub>-modified electrode exhibits a significantly higher current response, indicating better capacitance. Faradaic redox reactions can account for the charge storage mechanism of the Co<sub>3</sub>O<sub>4</sub> electrode[40], as shown by Equations (2) and (3).



In the process of charging, Co<sub>2</sub>O<sub>3</sub> absorbs electrons (6e<sup>-</sup>) and forms hydrated cobalt hydroxide species by reacting with hydroxide ions. In discharging, the hydrated cobalt hydroxide species transfers electrons (6e<sup>-</sup>) and proceeds oxidation back to Co<sub>3</sub>O<sub>4</sub>, releasing hydroxide ions. In 1M KOH and 1M Na<sub>2</sub>SO<sub>4</sub> electrolytes, the Co<sub>3</sub>O<sub>4</sub> electrode's electrochemical performance is displayed in Figure 7. For electrochemical performance in KOH electrolyte, the Co<sub>3</sub>O<sub>4</sub> electrode outperforms Na<sub>2</sub>SO<sub>4</sub>. Faster rates of K<sup>+</sup> ion intercalation and deintercalation are made possible by KOH's higher conductivity and ionic mobility, which makes sense[36]. The specific capacitance (Cs) values for the Co<sub>3</sub>O<sub>4</sub> electrode are 145, 95, 68, 47, 44, 36, and 31 Fg<sup>-1</sup>, respectively, for scan rates of 5, 10, 20, 50, 60, 80, and 100 mVs<sup>-1</sup> in 1M KOH. In 1M Na<sub>2</sub>SO<sub>4</sub>, the Cs values for the same scan speeds are 88, 58, 47, 34, 31, 25, and 21 Fg<sup>-1</sup>. The Cs decreases with increasing scan rate, which is consistent with the results displayed in Fig.7. Based on the cyclic voltammetry curves, the specific capacitance of the Co<sub>3</sub>O<sub>4</sub> electrode was calculated using Equation (4).

$$C_s = \frac{1}{\Delta v \times m} \int_{v_{min}}^{v_{max}} I(V) dv$$

where m is the mass of active CoO deposited (g), V is the scan rate (Vs<sup>-1</sup>), and Cs is the specific capacitance of the CoO electrode (Fg<sup>-1</sup>). In this equation, Cs stands for the Co<sub>3</sub>O<sub>4</sub> working electrode's specific capacitance (Fg<sup>-1</sup>), I for current density (A), Δt for discharge time (s), Δv for potential window (mVs<sup>-1</sup>), and m for the mass of active Co<sub>3</sub>O<sub>4</sub> deposited. Excellent cycle stability is essential for supercapacitor applications. As shown in Fig. 8, the Co<sub>3</sub>O<sub>4</sub> electrode exhibits long-term cyclic stability, retaining approximately 72% of the initial Cs after 500 cycles at a scan rate of 100 mVs<sup>-1</sup> in 1M KOH electrolyte.

To sum up, Co<sub>3</sub>O<sub>4</sub> nanoparticles show promise for use as an electrode material in alkaline electrolytes due to their greater specific capacitance values and faster charge-discharge rates when compared to neutral solutions.

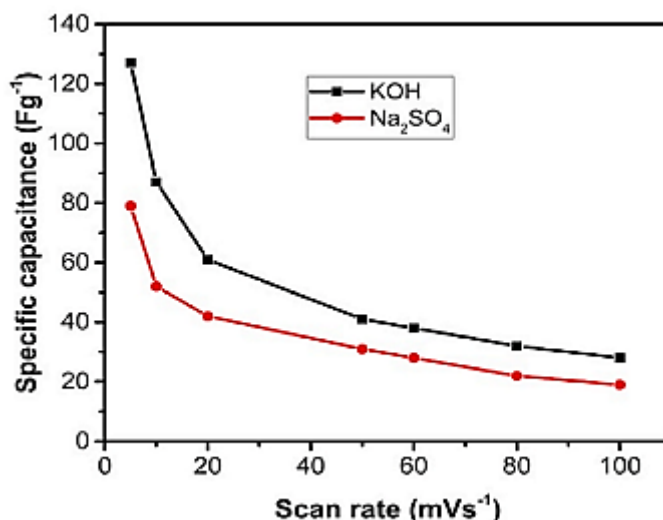


**Fig.7 Cs vs scan rates plot in KOH and Na<sub>2</sub>SO<sub>4</sub> electrolytes**

## 5. Conclusion

Co<sub>3</sub>O<sub>4</sub> nanoparticles synthesized by a straightforward hydrothermal process clearly show promising properties as electrode materials for supercapacitors, based on the thorough investigation reported in this study. The successful production of the cubic phase Co<sub>3</sub>O<sub>4</sub> with distinctive Co-O bonds and a non-uniform aggregation of nanoparticles was confirmed by the structural and morphological investigations. While surface wettability studies revealed the hydrophilic character of the Co<sub>3</sub>O<sub>4</sub> nanoparticles, which is advantageous for electrolyte interaction, the BET analysis yielded important information on the surface area and pore structure. Co<sub>3</sub>O<sub>4</sub> nanoparticles on carbon cloth (CC) showed remarkable specific capacitances of 132 Fg<sup>-1</sup> in KOH and 79 Fg<sup>-1</sup> in Na<sub>2</sub>SO<sub>4</sub> solutions when used as electrodes in supercapacitors. With almost 75% of their capacitance remaining after 500 cycles in KOH, the electrodes also demonstrated remarkable cycling stability, underscoring their durability and long-term usability. These results highlight the potential of Co<sub>3</sub>O<sub>4</sub> nanoparticles as cutting-edge materials with great performance and stability as supercapacitor electrodes. The work opens the door for additional Co<sub>3</sub>O<sub>4</sub>-based nanomaterial optimization and use in energy storage technologies.

## References

1. Khan, I., K. Saeed, and I. Khan, *Nanoparticles: Properties, applications and toxicities*. Arabian journal of chemistry, 2019. **12**(7): p. 908-931.
2. Goemann, H. and C. Feldmann, *Nanoparticulate functional materials*. Angewandte Chemie International Edition, 2010. **49**(8): p. 1362-1395.
3. Ealia, S.A.M. and M.P. Saravanakumar. *A review on the classification, characterisation, synthesis of nanoparticles and their application*. in *IOP conference series: materials science and engineering*. 2017. IOP Publishing.
4. Heiligtag, F.J. and M. Niederberger, *The fascinating world of nanoparticle research*. Materials today, 2013. **16**(7-8): p. 262-271.
5. Yan, J., et al., *Recent advances in design and fabrication of electrochemical supercapacitors with high energy densities*. Advanced Energy Materials, 2014. **4**(4): p. 1300816.
6. Zuo, W., et al., *Battery-supercapacitor hybrid devices: recent progress and future prospects*. Advanced science, 2017. **4**(7): p. 1600539.
7. Muzaffar, A., et al., *A review on recent advances in hybrid supercapacitors: Design, fabrication and applications*. Renewable and sustainable energy reviews, 2019. **101**: p. 123-145.
8. Yaseen, M., et al., *A review of supercapacitors: materials design, modification, and applications*. Energies, 2021. **14**(22): p. 7779.
9. Wang, X., et al., *Recent advance in Co<sub>3</sub>O<sub>4</sub> and Co<sub>3</sub>O<sub>4</sub>-containing electrode materials for high-performance supercapacitors*. Molecules, 2020. **25**(2): p. 269.
10. Kumar, S., et al., *Metal oxides for energy applications*, in *Colloidal Metal Oxide Nanoparticles*. 2020, Elsevier. p. 471-504.
11. Pang, H., et al., *Synthesis of functional nanomaterials for electrochemical energy storage*. 2020: Springer.
12. Kokila, G., C. Mallikarjunaswamy, and V.L. Ranganatha, *A review on synthesis and applications of versatile nanomaterials*. Inorganic and Nano-Metal Chemistry, 2022: p. 1-30.
13. Salem, S.S., et al., *A comprehensive review of nanomaterials: Types, synthesis, characterization, and applications*. Biointerface Res. Appl. Chem, 2022. **13**(1): p. 41.
14. Abouali, S., et al., *Electrospun carbon nanofibers with in situ encapsulated Co<sub>3</sub>O<sub>4</sub> nanoparticles as electrodes for high-performance supercapacitors*. ACS applied materials & interfaces, 2015. **7**(24): p. 13503-13511.
15. Meng, T., et al., *Co<sub>3</sub>O<sub>4</sub> nanorods with self-assembled nanoparticles in queue for supercapacitor*. Electrochimica Acta, 2015. **180**: p. 104-111.
16. Liu, F., et al., *Facile synthesis of ultrafine cobalt oxide nanoparticles for high-performance supercapacitors*. Journal of colloid and interface science, 2017. **505**: p. 796-804.
17. Kim, B.K., et al., *Electrochemical supercapacitors for energy storage and conversion*. Handbook of clean energy systems, 2015: p. 1-25.
18. Zhao, J. and A.F. Burke, *Electrochemical capacitors: Materials, technologies and performance*. Energy Storage Materials, 2021. **36**: p. 31-55.

19. Gupta, P., et al., *Recent developments and research avenues for polymers in electric vehicles*. The Chemical Record, 2022. **22**(11): p. e202200186.
20. Nassar, M.Y., *Size-controlled synthesis of CoCO<sub>3</sub> and Co<sub>3</sub>O<sub>4</sub> nanoparticles by free-surfactant hydrothermal method*. Materials letters, 2013. **94**: p. 112-115.
21. Xu, J., et al., *Preparation and electrochemical capacitance of cobalt oxide (Co<sub>3</sub>O<sub>4</sub>) nanotubes as supercapacitor material*. Electrochimica Acta, 2010. **56**(2): p. 732-736.
22. Aghazadeh, M., et al., *High performance pseudocapacitor electrode material fabricated by pulse electro-synthesized cobalt oxide nanostructures*. International Journal of Electrochemical Science, 2016. **11**(12): p. 11016-11027.
23. Umar, A., et al., *Perforated Co<sub>3</sub>O<sub>4</sub> nanosheets as high-performing supercapacitor material*. Electrochimica Acta, 2021. **389**: p. 138661.
24. Saikia, B.K., et al., *A brief review on supercapacitor energy storage devices and utilization of natural carbon resources as their electrode materials*. Fuel, 2020. **282**: p. 118796.
25. Biswas, S. and A. Chowdhury, *Organic supercapacitors as the next generation energy storage device: emergence, opportunity, and challenges*. ChemPhysChem, 2023. **24**(3): p. e202200567.
26. Kaviyarasu, K., A. Raja, and P.A. Devarajan, *Structural elucidation and spectral characterizations of Co<sub>3</sub>O<sub>4</sub> nanoflakes*. Spectrochimica Acta Part A: Molecular and Biomolecular Spectroscopy, 2013. **114**: p. 586-591.
27. Yang, Y.-p., et al., *Preparation and electrochemical performance of nanosized Co<sub>3</sub>O<sub>4</sub> via hydrothermal method*. Transactions of Nonferrous Metals Society of China, 2007. **17**(6): p. 1334-1338.
28. Deori, K., et al., *Morphology controlled synthesis of nanoporous Co<sub>3</sub>O<sub>4</sub> nanostructures and their charge storage characteristics in supercapacitors*. ACS applied materials & interfaces, 2013. **5**(21): p. 10665-10672.
29. Jamil, S., M.R.S.A. Janjua, and S.R. Khan, *Synthesis and structural investigation of polyhedron Co<sub>3</sub>O<sub>4</sub> nanoparticles: Catalytic application and as fuel additive*. Materials Chemistry and Physics, 2018. **216**: p. 82-92.
30. Andrade-Sanchez, M., et al., *Temperature and pH effect on reaction mechanism and particle size of nanostructured Co<sub>3</sub>O<sub>4</sub> thin films obtained by sol-gel/dip-coating*. Materials Research Express, 2021. **8**(2): p. 025015.
31. El-Shamy, O.A. and M.A. Deyab, *The most popular and effective synthesis processes for Co<sub>3</sub>O<sub>4</sub> nanoparticles and their benefit in preventing corrosion*. Zeitschrift für Physikalische Chemie, 2023. **237**(3): p. 333-350.
32. Kumarage, G.W. and E. Comini, *Low-dimensional nanostructures based on cobalt oxide (Co<sub>3</sub>O<sub>4</sub>) in chemical-gas sensing*. Chemosensors, 2021. **9**(8): p. 197.
33. Wang, S., et al., *One-dimensional porous Co<sub>3</sub>O<sub>4</sub> rectangular rods for enhanced acetone gas sensing properties*. Sensors and Actuators B: Chemical, 2019. **297**: p. 126746.
34. Zheng, M.-b., et al., *Preparation of mesoporous Co<sub>3</sub>O<sub>4</sub> nanoparticles via solid-liquid route and effects of calcination temperature and textural parameters on their electrochemical capacitive behaviors*. The Journal of Physical Chemistry C, 2022. **113**(9): p. 3887-3894.
35. Pudukudy, M., et al., *Facile synthesis of bimodal mesoporous spinel Co<sub>3</sub>O<sub>4</sub> nanomaterials and their structural properties*. Superlattices and Microstructures, 2019. **64**: p. 15-26.
36. Jadhav, S.L., et al., *Influence of deposition current and different electrolytes on charge storage performance of Co<sub>3</sub>O<sub>4</sub> electrode material*. Journal of Physics and Chemistry of Solids, 2023. **180**: p. 111422.
37. Rajeshkhanna, G., E. Umeshbabu, and G.R. Rao, *Charge storage, electrocatalytic and sensing activities of nest-like nanostructured Co<sub>3</sub>O<sub>4</sub>*. Journal of Colloid and Interface Science, 2017. **487**: p. 20-30.
38. Zhao, L., et al., *Electrolyte-wettability issues and challenges of electrode materials in electrochemical energy storage, energy conversion, and beyond*. Advanced Science, 2023. **10**(17): p. 2300283.
39. Adhikari, H., *Synthesis and Electrochemical Performance of Hydrothermally Synthesized Co<sub>3</sub>O<sub>4</sub> Nanostructured Particles*. 2020.
40. Adekunle, A.S., *Electrochemical and electrocatalytic properties of carbon nanotubes integrated with selected metal and metal oxide nanoparticles*. 2019, University of Pretoria.